Wide optical spectrum range, subvolt, compact modulator based on an electro-optic polymer refilled silicon slot photonic crystal waveguide

Xingyu Zhang,[1,4,†] Amir Hosseini,[2,*,†] Swapnajit Chakravarty,[2] Jingdong Luo,[3] Alex K.-Y. Jen,[3] and Ray T. Chen[1,5]

[1]*Microelectronics Research Center, Electrical and Computer Engineering Department, University of Texas at Austin, Austin, Texas 78758, USA*

[2]*Omega Optics, Inc., 10306 Sausalito Dr., Austin, Texas 78759, USA*

[3]*Department of Materials Science and Engineering, University of Washington, Seattle, Washington 98195, USA*

[4]*e-mail: xzhang@utexas.edu*

[5]*e-mail: raychen@uts.cc.utexas.edu*

**Corresponding author: amirh@utexas.edu*

Received July 17, 2013; revised October 16, 2013; accepted October 17, 2013; posted October 18, 2013 (Doc. ID 194007); published November 15, 2013

We design and demonstrate a compact and low-power, band-engineered, electro-optic (EO) polymer refilled silicon slot photonic crystal waveguide (PCW) modulator. The EO polymer is engineered for large EO activity and near-infrared transparency. A PCW step coupler is used for optimum coupling to the slow-light mode of the band-engineered PCW. The half-wave switching voltage is measured to be $V_\pi = 0.97 \pm 0.02$ V over an optical spectrum range of 8 nm, corresponding to the effective in-device r_{33} of 1190 pm/V and $V_\pi \times L = 0.291 \pm 0.006$ V × mm in a push–pull configuration. Excluding the slow-light effect, we estimate that the EO polymer is poled with an efficiency of 89 pm/V in the slot. © 2013 Optical Society of America

OCIS codes: (230.4110) Modulators; (130.5296) Photonic crystal waveguides; (250.2080) Polymer active devices.
http://dx.doi.org/10.1364/OL.38.004931

Electro-optic (EO) polymer modulators in optical links are promising for low-power consumption [1] and broad-bandwidth operation [2]. The EO coefficient (r_{33}) of EO polymers can be several times larger than that of lithium niobate. In addition to conventional all-polymer devices [1,2], combination of silicon photonics and EO polymer has shown to enable compact and high-performance integrated devices [3], such as slot waveguide Mach–Zehnder interferometer (MZI) modulators [4], slot waveguide ring-resonator modulators [5], and slot photonic crystal waveguide (PCW) modulators [6]. The fabrication process of these devices involves the poling of the EO polymer at an elevated temperature. Unfortunately, the leakage current due to the charge injection through the silicon–polymer interface significantly reduces the poling efficiency in narrow-slot waveguides (slot width, $S_w < 200$ nm). Among the aforementioned structures, slot PCWs can support the optical mode for S_w as large as 320 nm [7]. Such a wide slot was shown to reduce the leakage current by two orders of magnitude, resulting in 5× improvement in the in-device r_{33} compared with a slot PCW with $S_w = 75$ nm [7].

One problem that remains among slot PCW modulators is their narrow operating optical bandwidth of <1 nm [8–10] because of the high group velocity dispersion in the slow-light optical spectrum range. To broaden the operating optical bandwidth of PCW modulators, lattice-shifted PCWs can be employed, where the spatial shift of certain holes can modify the structure to provide low-dispersion slow light [11–15].

In this Letter, we report a symmetric MZI modulator based on a band-engineered slot PCW refilled with an EO polymer, SEO125 from Soluxra, LLC. SEO125 exhibits exceptional combination of large EO activity, low optical loss, and good temporal stability. The r_{33} value of its poled thin films is around 125 pm/V at a wavelength of 1310 nm, which is measured by the Teng–Man reflection technique. The design and synthesis of SEO125 encompasses recent development of highly efficient nonlinear optical chromophores with a few key molecular and material parameters, including large β values, good near-infrared transparency, excellent chemical and photostability, and improved processability in polymers [16]. Using a band-engineered, EO polymer refilled slot PCW with $S_w = 320$ nm, we demonstrate a slow-light-enhanced effective in-device r_{33} of 1190 pm/V over an 8 nm optical spectrum range. Excluding the slow-light effect, we estimate an in-device material r_{33} of 89 pm/V for SEO125 in the slot that shows 51% improvement compared with the results (59 pm/V) in [7].

A schematic of the device on silicon on insulator (SOI) (Si thickness = 250 nm, oxide thickness = 3 μm) is shown in Fig. 1(a). The input and output strip waveguides are connected to the device using a strip waveguide to slot waveguide mode converter. PCW couplers consisting of a fast-light section [17] connect the mode converters to a 300 μm long slow-light PCW section. The slow-light PCW section is band-engineered by lateral shifting of the first three rows on the two sides of the slot [indicated by s_1, s_2, and s_3 in Fig. 1(a)] [12] and by varying the center-to-center distance between two rows adjacent to the slot [W in Fig. 1(a)]. Multimode interference couplers are used for beam splitting/combining [18]. Subwavelength gratings are designed to couple light into and out of the silicon strip [19].

For lattice constant $a = 425$ nm, it is found that with hole diameter $d = 300$ nm, $s_1 = 0$, $s_2 = -85$ nm, $s_3 = 85$ nm, $S_w = 320$ nm, and $W = 1.54(\sqrt{3})a$, we can achieve an average group index ($n_g = c/v_g$) of 20.4(±10%) over an 8.2 nm optical bandwidth. The PCW coupler

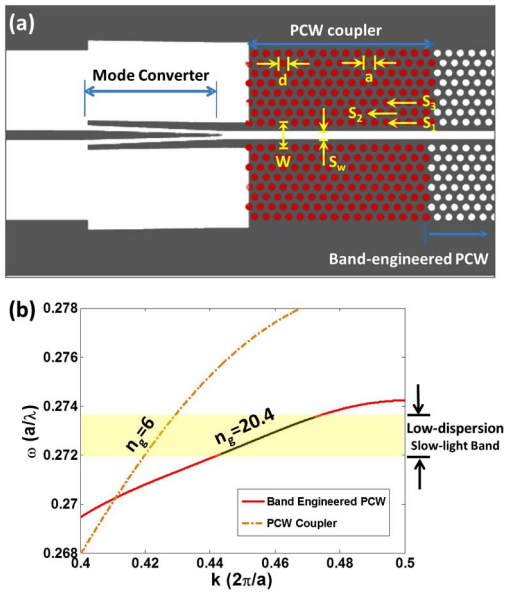

Fig. 1. (a) Layout of the PCW coupler (mode converter+PCW coupler). The black area corresponds to un-etched silicon. (b) Band diagram of the engineered slow-light PCW and the PCW coupler.

$[a = 425\ \text{nm},\quad d = 300\ \text{nm},\quad s_1 = 0,\quad s_2 = 0,\quad s_3 = 0,\ S_w = 320\ \text{nm},\ W = 1.45(\sqrt{3})a]$ consists of 16 periods and is designed for a low $n_g = 6$ over the same wavelength range. The band diagrams of the slow-light and fast-light PCWs are shown in Fig. 1(b).

The fabrication procedure starts with an SOI wafer with 250 nm thick top silicon. All photonic circuitries are fabricated by electron beam lithography and reactive-ion etching in a single patterning/etching step, whereas the gold electrodes are patterned by photolithography and a lift-off process, as shown in Figs. 2(a) and 2(b). The EO polymer, SEO125, is infiltrated into the slot PCW by spin coating. The silicon PCW regions including holes and the slot are fully covered by the EO polymer, as shown in the SEM image in Figs. 2(c) and 2(d). A microscope image of the fabricated MZI is shown in Fig. 3(a). Next, the sample is poled by an electric field of 100 V/μm in a push–pull configuration at the glass transition

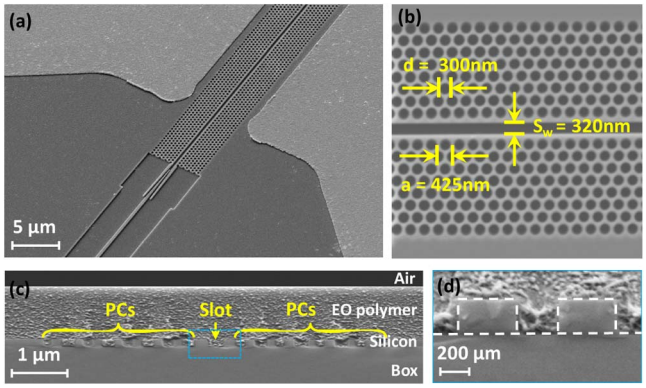

Fig. 2. Scanning electron microscopy (SEM) images of the fabricated device. (a) Tiled view of a local area of the silicon slot PCW modulator. (b) Top view of the slot PCW area. (c) Cross-sectional view of the EO polymer refilled silicon slot PCW. PCs, photonic crystals. (d) Zoom-in image of the dashed square area in (c).

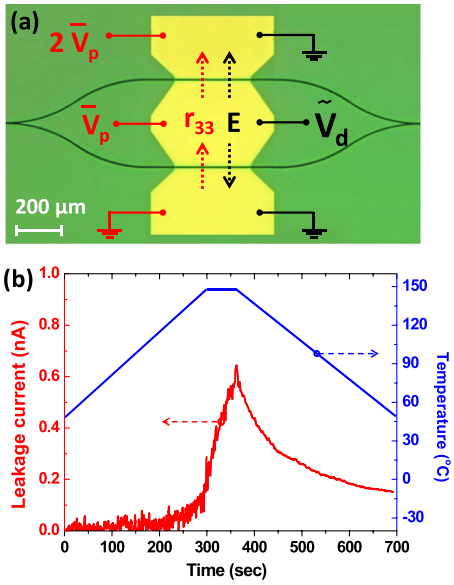

Fig. 3. (a) Top view of fabricated slot PCW MZI modulator. The red circuit connection indicates the push–pull poling configuration and the induced r_{33} direction, and the black circuit connection indicates the modulation configuration. V_p, poling voltage; V_d, diving voltage. (b) The temperature-dependent leakage current in the EO polymer poling process.

temperature ($T_g = 145°\text{C}$) of the EO polymer. The leakage current as well as the hot plate temperature are monitored and are shown in Fig. 3(b). It can be seen that the maximum leakage current remains below 0.659 nA, corresponding to a leakage current density of 8.79 A/m^2 [$= 0.659\ \text{nA}/(300\ \mu\text{m} * 250\ \text{nm})$)]. For comparison, the typical leakage current density of the EO polymer is 1–10 A/m^2 in a thin-film configuration. This poling result is repeatable and shows that the 320 nm wide slot dramatically reduces the leakage current that is known to be detrimental to the poling efficiency [20].

For modulation test, TE-polarized light from a tunable laser source (1550 nm, 2.5 mW) is coupled into and out of the device through grating couplers. The total optical insertion loss is 20 dB, including the 6.5 dB per facet coupling loss from grating couplers. RF signals are applied to the electrodes as shown in Fig. 3(a). The modulator is biased at the 3 dB point and driven by a 100 kHz triangular RF wave with a peak-to-peak voltage of 1.4 V. The modulated output optical signal is sent to a photodetector and then displayed on a digital oscilloscope. The modulation frequency is within the bandwidth of the photodetector and the oscilloscope. From the output optical waveform measured by the digital oscilloscope, overmodulation is observed. The V_π of the modulator is measured to be 0.973 V from the transfer function of the overmodulated optical signal and the input RF signal on the oscilloscope, by finding the difference between the applied voltage at which the optical output is at a maximum and the voltage at which the optical output is at the following minimum [1,3,7,20,21]. The effective in-device r_{33} is then calculated to be

$$r_{33\text{-effective}} = \frac{\lambda S_w}{n^3 V_\pi \sigma L} = 1190\ \frac{\text{pm}}{\text{V}}, \tag{1}$$

where $\lambda = 1.55$ μm, $S_w = 320$ nm, $n = 1.63$, $L = 300$ μm, and $\sigma = 0.33$ (confinement factor in the slot) as calculated by simulation. This extraordinarily high r_{33} value confirms the combined enhancing effects of slow light and an improved poling efficiency. This band-engineered 320 nm slot PCW modulator also achieves very high modulation efficiency with $V_\pi \times L = 0.973$ V × 300 μm = 0.292 V × mm.

We also estimate the actual in-device r_{33} excluding the slow-light effect using [11]

$$L = \frac{\lambda}{2\sigma n_g}\left(\frac{n}{\Delta n}\right), \tag{2}$$

where $\Delta n = n^3 r_{33} V_\pi/(2S_w)$. The estimated in-device r_{33} is 89 pm/V, which is significantly larger than that in our previous work in [7] and is the highest poling efficiency demonstrated in a slot waveguide, to the best of our knowledge. Considering the r_{33} dispersion from the two-level model approximation [22], this value also represents nearly 100% poling efficiency that has been obtained in poled thin films of SEO125.

To demonstrate the wide optical spectrum range, the optical wavelength is tuned from 1544 to 1560 nm while all other testing conditions are fixed. The V_π measured at different wavelength, as well as the corresponding calculated effective in-device r_{33}, is plotted in Fig. 4(a). It can be seen that V_π is nearly constant, that is, 0.97 ± 0.02 V, over the optical spectrum range of 8 nm (low-dispersion slow-light region: from 1546.5 to 1554.5 nm), corresponding to the effective in-device r_{33} of 1190 pm/V and $V_\pi \times L$ of 0.291 ± 0.006 V × mm. We note that this $V_\pi \times L$ value is relative to a push–pull configuration. Relative to a single-arm modulator where the effective length of the MZI is the length of both arms together, $V_\pi \times (2L) = 0.582 \pm 0.012$ V × mm is still a record low value.

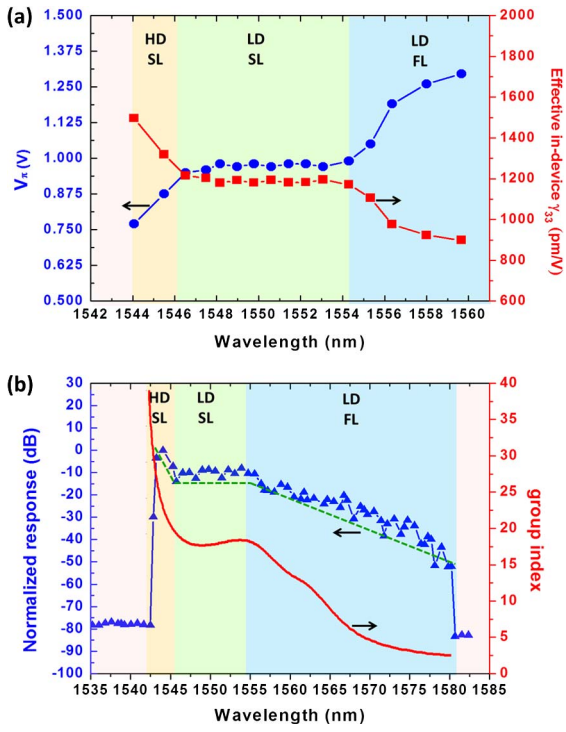

Fig. 4. (a) Measured V_π and corresponding calculated effective in-device r_{33} versus wavelength (at 100 kHz). HD SL, high-dispersion slow light; LD SL, low-dispersion slow light; LD FL, low-dispersion fast light. (b) Normalized device response versus wavelength (at 100 kHz). The green dashed line indicates the trend of the response change over different wavelength. The simulated n_g versus wavelength is also overlaid.

Furthermore, a small signal modulation test is done at $V_{pp} < 1$ V over a range of wavelength from 1535 to 1582 nm, while all other testing conditions remain the same. The modulated optical signal is converted to an electrical signal by a photodetector and then measured by a microwave spectrum analyzer. The wavelength dependence of the normalized modulated optical signal is plotted in Fig. 4(b). It can be seen that the defect-guided mode of the slot PCW occurs from 1543 to 1580 nm. Maximum response occurs at the high-dispersion slow-light region (wavelength from 1543 to 1546.5 nm), because of the largest slow-light enhancement (largest n_g) in this region. The response is almost flat in the low-dispersion slow-light region (wavelength from 1546.5 to 1554.5 nm), because the slot PCW is band-engineered to have a nearly constant n_g in this wavelength range. As the optical signal is tuned to a longer wavelength (low-dispersion fast-light region: from 1554.5 to1580 nm), the device response becomes smaller due to decreasing n_g.

In summary, we have designed, fabricated, and characterized a band-engineered, EO polymer refilled silicon slot PCW MZI modulator. The half-wave switching voltage is measured to be $V_\pi = 0.97 \pm 0.02$ V over an optical spectrum range of 8 nm, corresponding to the slow-light-enhanced effective in-device r_{33} of 1190 pm/V and $V_\pi \times L$ of 0.291 ± 0.006 V × mm. Excluding the slow-light effect, we estimate that the EO polymer is poled with a record high EO activity of 89 pm/V in the slot at a wavelength of 1.55 μm. In our future work, the optical loss of our modulator can be reduced further, such as by design of low-loss PCW couplers [23] and improved coupling and packaging methods [24]. Photochemical stability, a common issue of polymer-based modulators, is expected to be improved by hermetically sealing the EO polymer by robust packaging [25,26]. Poled thin films of SEO125 have shown good temporal stability due to its relatively high $T_g = 145$°C, and after poling its EO coefficients were essentially unchanged under ambient conditions. Whereas SEO125 is a newly developed material and its complete characterization in terms of performance and photostability is an ongoing effort, EO polymers with similar compositions have been demonstrated to have potential long-term stability by removing oxygen in the packaging of devices [27].

The authors would like to acknowledge the Air Force Research Laboratory (AFRL) for supporting this work under the Small Business Technology Transfer Research (STTR) program (Grant No. FA8650-12-M-5131) monitored by Dr. Robert Nelson and Dr. Charles Lee.

†These authors contributed equally to this work.

References

1. Y. Shi, C. Zhang, H. Zhang, J. H. Bechtel, L. R. Dalton, B. H. Robinson, and W. H. Steier, Science **288**, 119 (2000).

2. D. Chen, H. R. Fetterman, A. Chen, W. H. Steier, L. R. Dalton, W. Wang, and Y. Shi, Appl. Phys. Lett. **70**, 3335 (1997).
3. X. Zhang, A. Hosseini, X. Lin, H. Subbaraman, and R. T. Chen, IEEE J. Sel. Top. Quantum Electron. **19**, 3401115 (2013).
4. R. Ding, T. Baehr-Jones, W.-J. Kim, A. Spott, M. Fournier, J.-M. Fedeli, S. Huang, J. Luo, A. K.-Y. Jen, and L. Dalton, J. Lightwave Technol. **29**, 1112 (2011).
5. M. Gould, T. Baehr-Jones, R. Ding, S. Huang, J. Luo, A. K.-Y. Jen, J.-M. Fedeli, M. Fournier, and M. Hochberg, Opt. Express **19**, 3952 (2011).
6. J. H. Wülbern, S. Prorok, J. Hampe, A. Petrov, M. Eich, J. Luo, A. K.-Y. Jen, M. Jenett, and A. Jacob, Opt. Lett. **35**, 2753 (2010).
7. X. Wang, C.-Y. Lin, S. Chakravarty, J. Luo, A. K.-Y. Jen, and R. T. Chen, Opt. Lett. **36**, 882 (2011).
8. H. C. Nguyen, Y. Sakai, M. Shinkawa, N. Ishikura, and T. Baba, Opt. Express **19**, 13000 (2011).
9. J. H. Wulbern, J. Hampe, A. Petrov, M. Eich, J. Luo, A. K.-Y. Jen, A. Di Falco, T. F. Krauss, and J. Bruns, Appl. Phys. Lett. **94**, 241107 (2009).
10. H. C. Nguyen, Y. Sakai, M. Shinkawa, N. Ishikura, and T. Baba, IEEE J. Quantum Electron. **48**, 210 (2012).
11. A. Hosseini, X. Xu, H. Subbaraman, C.-Y. Lin, S. Rahimi, and R. T. Chen, Opt. Express **20**, 12318 (2012).
12. S. Rahimi, A. Hosseini, X. Xu, H. Subbaraman, and R. T. Chen, Opt. Express **19**, 21832 (2011).
13. Y. Hamachi, S. Kubo, and T. Baba, Opt. Lett. **34**, 1072 (2009).
14. S. Schulz, L. O'Faolain, D. Beggs, T. White, A. Melloni, and T. Krauss, J. Opt. **12**, 104004 (2010).
15. A. Y. Petrov and M. Eich, Appl. Phys. Lett. **85**, 4866 (2004).
16. J. Luo, X.-H. Zhou, and A. K.-Y. Jen, J. Mater. Chem. **19**, 7410 (2009).
17. A. Hosseini, X. Xu, D. N. Kwong, H. Subbaraman, W. Jiang, and R. T. Chen, Appl. Phys. Lett. **98**, 031107 (2011).
18. A. Hosseini, D. Kwong, C.-Y. Lin, B. S. Lee, and R. T. Chen, IEEE J. Sel. Top. Quantum Electron. **16**, 61 (2010).
19. X. Xu, H. Subbaraman, J. Covey, D. Kwong, A. Hosseini, and R. T. Chen, Appl. Phys. Lett. **101**, 031109 (2012).
20. X. Zhang, B. Lee, C.-y. Lin, A. X. Wang, A. Hosseini, and R. T. Chen, IEEE Photon. J. **4**, 2214 (2012).
21. C.-Y. Lin, X. Wang, S. Chakravarty, B. S. Lee, W. Lai, J. Luo, A. K.-Y. Jen, and R. T. Chen, Appl. Phys. Lett. **97**, 093304 (2010).
22. C. Greenlee, A. Guilmo, A. Opadeyi, R. Himmelhuber, R. A. Norwood, M. Fallahi, J. Luo, S. Huang, X.-H. Zhou, and A. K.-Y. Jen, Appl. Phys. Lett. **97**, 041109 (2010).
23. R. Palmer, L. Alloatti, D. Korn, W. Heni, P. C. Schindler, J. Bolten, M. Karl, M. Waldow, T. Wahlbrink, W. Freude, C. Koos, and J. Leuthold, IEEE Photon. J. **5**, 2200409 (2013).
24. B. Snyder and P. O'Brien, "Planar fiber packaging method for silicon photonic integrated circuits," in *Optical Fiber Communication Conference and Exposition (OFC/NFOEC), 2012 and the National Fiber Optic Engineers Conference* (IEEE, 2012), pp. 1–3.
25. R. Dinu, D. Jin, G. M. Yu, B. Q. Chen, D. Y. Huang, H. Chen, A. Barklund, E. Miller, C. L. Wei, and J. Vemagiri, J. Lightwave Technol. **27**, 1527 (2009).
26. D. Jin, H. Chen, A. Barklund, J. Mallari, G. Yu, E. Miller, and R. Dinu, Proc. SPIE **7599**, 75990H (2010).
27. S. Takahashi, B. Bhola, A. Yick, W. H. Steier, J. Luo, A. K.-Y. Jen, D. Jin, and R. Dinu, J. Lightwave Technol. **27**, 1045 (2009).